Intentionally vs. Spontaneously Prolonged Gaze: A MEG Study of Active Gaze-Based Interaction

A.N. Vasilyev[1,2 *], E.P. Svirin[1], I.A. Dubynin[1], A.V. Butorina[1,3,4], Y.O. Nuzhdin[5], A.E. Ossadtchi[1,4,6], T.A. Stroganova[1], S.L. Shishkin[1]

[1] MEG Center (Center for Neurocognitive Research), Moscow State University of Psychology and Education, Moscow, Russian Federation
[2] Department of Human and Animal Physiology, Lomonosov Moscow State University, Moscow, Russian Federation
[3] Center for Neurobiology and Neurorehabilitation, Skolkovo Institute of Science and Technology, Moscow, Russian Federation
[4] LLC "Life Improvement by Future Technologies Center", Moscow, Russian Federation
[5] Independent Researcher, Eindhoven, the Netherlands
[6] Center for Bioelectric Interfaces, Higher School of Economics, Moscow, Russian Federation

Abstract

Eye fixations are increasingly used to control computers through gaze-sensitive interfaces, yet the brain mechanisms underlying this non-visual use of gaze remain poorly understood. In this study, we recorded 306-channel magnetoencephalography (MEG) signals while participants played a video game controlled by their eye movements. Each move required selecting an object by fixating on it for at least 500 ms. Gaze dwells were classified as intentional if followed by a confirmation gaze on a special location and as spontaneous otherwise. In contrast to previous EEG studies on gaze-based interaction, we identified both oscillatory and sustained phase-locked MEG activity differentiating intentional and spontaneous gaze dwells, emerging near dwell onset and persisting until its termination. Thus, despite the apparent ease of controlling eye movements for gaze-based interaction, this process engages distinct neural signatures detectable with MEG, which are only partially similar to those observed in tasks requiring explicit inhibition of prepotent oculomotor responses. These findings highlight that contrasting spontaneous and intentional gaze dwells collected during free-behavior gaze-based interaction can serve as a novel methodology for studying mechanisms of voluntary control. Unlike traditional tasks in voluntary eye movement research, this approach avoids unnatural efforts from participants, offering a more naturalistic context for investigation.

Keywords: eigendecomposition, fixations, frontal eye fields, oscillations, voluntary control.

Running title: MEG study of intentionally prolonged gaze

[*] Corresponding author. Email: a.vasilyev@anvmail.com

Introduction

Gaze-based communication and control represent a promising approach for hands-free interaction with computers and other devices, been in development for more than three decades (Duchowski 2018). It is particularly beneficial for paralyzed individuals (Majaranta 2011), but also can be used by healthy people, especially as an effective input in virtual, augmented and mixed reality (VR/AR/MR) (O'Callaghan 2024; Plopski et al. 2022). To issue a command, a user of this technology typically keeps their gaze on a “gaze-sensitive” element of a graphical interface, such as a screen button, for a relatively short period (Duchowski 2018; Majaranta 2011). An eye tracker captures the gaze position, and when the gaze dwell time in the vicinity of a screen button exceeds a specified threshold, the button is activated. The action is similar to pressing a computer mouse button or tapping on a touchscreen but involves a temporal freezing of the natural spontaneous gaze behavior.

Despite the growing interest in gaze-based human-computer interaction, the brain mechanisms underlying eye movement control in this context have received little attention, likely because this interaction has been considered primarily an engineering challenge. However, gaze-based interaction has unique characteristics that distinguish it from other forms of voluntary behavior. First, the "stillness-based" nature of gaze-based interaction is in stark contrast to typical manual actions, which involve intentional movement. In everyday scenarios, hands remain still by default, whereas the default state for eyes is their frequent motion (primarily through saccades). Secondly, intentional gaze dwells[1] used in gaze-based interaction represent a rare example of voluntary control executed with minimal effort. Thus, studying the physiological mechanisms specifically related to gaze-based control may enhance this technology. Moreover, using gaze-based actions as a model of voluntary actions could also provide insights into the brain's mechanisms of voluntary control in general.

[1] We use the term *dwell* for the events of relatively long stay of gaze in a designated area (area of interest). Such events are often called *fixations*, especially in the literature on gaze-based interaction, but they do not need to fit strict definitions of an eye fixation used in the eye movement literature. Moreover, a dwell may include more than one fixation (in strict definition) and other kinds of eye movement.

Voluntary control of eye movement has been extensively studied in brain research, usually involving salient visual stimuli. In these studies, participants may be required to make voluntary saccades in different directions (often opposite to the stimulus), as in the antisaccade task (Funahashi et al. 1993; Hallett 1978; Munoz and Everling 2004), or to maintain a gaze fixation despite an urge to make a saccade, as seen in response inhibition paradigms like the NoGo task (Brown et al. 2006; Brown et al. 2008; Isoda and Hikosaka 2007) and in delayed antisaccade and prosaccade tasks (e.g., (Ettinger et al. 2008)). These tasks typically impose stronger control demands than most everyday activities, likely leading to exaggeration of voluntary control effects and even to contamination of effects related to voluntary control with effects related to effort (Jarvstad and Gilchrist 2019). To alleviate this problem, Jarvstad and Gilchrist (2019) proposed a novel, less demanding paradigm for studying saccade control. Notably, their design included long fixations as a baseline (20 seconds), which itself required a significant cognitive effort from the participants. In contrast, dwell time is usually set much shorter in gaze-interaction interfaces to avoid user discomfort (often 1 second or less).

Instructions to avoid natural gaze behavior and to keep gaze still on some object for uncomfortably long time are not uncommon, even in baseline conditions, also in psychological and neurophysiological studies that do not target voluntary control of eye movement.

The gaze-based interaction paradigm could help in the exploration of the fundamental mechanisms of voluntary control. Intuitively, voluntary brain control of gaze dwells used for interacting with computers should differ from the brain control of similarly timed spontaneous dwells occurring under the same visual conditions. At the same time, as cognitive effort is low even for intentional dwells in this context, any difference in brain activation related to intentional versus spontaneous dwells during gaze-based interaction may be attributed more specifically to the voluntary components of eye movement control than in traditional paradigms.

Understanding the brain mechanisms of low-effort voluntary control of eye movements could be important not only for basic neuroscience but also for advancing gaze-based interaction technology. Specifically, it could help address the so-called Midas touch problem, i.e., the inability of a gaze-

sensitive interface to distinguish between eye movement patterns intentionally used to send a command from similar patterns that occur spontaneously, without intent (Jacob 1990). In particular, when an interface is made sensitive to long dwells, unwanted responses to dwells that are long due to automatic, unconscious functioning of eye movement control are inevitable. Countermeasures against the Midas touch problem require additional user effort (Majaranta and Bulling 2014; Velichkovsky et al. 1997). Learning the difference between the intentional and spontaneous gaze dwells could help to obtain, from brain signals, markers that would indicate which dwells are intentional and require a response from the interface (Ihme and Zander 2011; Protzak et al. 2013).

A straightforward way to study the difference between the intentional and spontaneous gaze dwells is collecting them from participants who solve some tasks using a gaze-based human-computer interface (Shishkin et al. 2016a). The task and the visual display should provoke sufficient number of spontaneous gaze dwells with duration exceeding the dwell time threshold used in the interaction. To this end, Shishkin et al. (2016b) developed a gaze-controlled game and recorded the electroencephalogram (EEG) when participants played it. Labeling intentional and spontaneous dwells was based on the rule that required switch on gaze-based control prior to each move using a dwell at a designated screen position ("switch-on button"). Intentional dwells were shown to be characterized by a gradually mounting EEG activity in their latter portion, likely related to the anticipation of the interface triggering (Shishkin et al. 2016b). However, this EEG marker seemed to be not specific to intentionality of a dwell (e.g., it could be developed also in spontaneous but perceived gaze dwells if they could lead to unwanted interface triggering, as was likely the case in our online study (Nuzhdin et al. 2017)). The earlier time interval, unfortunately, could not be effectively studied due to the high difference in eye movement pattern prior to the dwell, which was determined using the "switch-on button".

In the current study, we addressed whether voluntarily prolonged gaze dwells used to control a computer are accompanied by distinct brain activity, not found or at least less pronounced in spontaneous long dwells, already from their onset. We used the same gaze-controlled game as in (Shishkin et al. 2016b) but modified the gaze-based control rules to minimize the influence of preceding events on the time

interval of intentional dwells. Most of the game rules remained unchanged, as they provided a basis for comfortable interaction and stable motivation in the previous study. Instead of recording the EEG, we co-registered 306-channel magnetoencephalography (MEG) data with eye-tracking data. A special procedure for selecting intentional and spontaneous dwells was developed to ensure contrast on the "voluntariness" scale. The dataset collected in this study has been used previously to assess the usefulness of MEG data for classifying spontaneous and intentional gaze dwells, with a simpler procedure of labeling the intentional and spontaneous dwells (Ovchinnikova et al. 2021).

We hypothesized that certain MEG components would be more pronounced in intentional gaze dwells compared to spontaneous dwells early in their time course, indicating their specific relation to voluntary control. A priori, we could not be certain about the possible locations of such effects; therefore, a whole-head analysis was planned instead of a region-of-interest (ROI)-based one. We identified MEG components phase-locked to dwell onset and non-phase-locked oscillatory MEG components that differed between intentional and spontaneous gaze dwells early in their course.

Method

Participants

A total of 32 healthy participants (18-51 years, mean age 25 years; 12 female) were recruited for the study. Among them, seven had previously participated in experiments using the same gaze-controlled game, although with a different sequence of required eye fixations for making moves. The study was conducted in compliance with the Helsinki Declaration and received approval from the ethical committee of Moscow State University of Psychology and Education. All participants provided written informed consent. During the initial stages of data labeling, three participants (two female and one male) were excluded due to insufficient data (fewer than 50 intentional dwells), leaving a final sample of 29 participants for analysis.

Experimental setup

The experiments were conducted in a magnetically shielded room at the MEG Center (Center for Neurocognitive Research), Moscow State University of Psychology and Education, Russia (http://megmoscow.com/). Participants were seated comfortably in an upright position during the MEG recording. Visual stimuli were presented using a digital light processing projector (Panasonic PT-D7700E-K) with a resolution of 1280 × 1024, projected onto a translucent screen positioned 1.42 meters from the participants' eyes.

MEG recording

MEG data were recorded using a 306-channel Elekta Neuromag TRIUX™ system (MEGIN/Elekta Oy, Helsinki, Finland) while participants were seated. This system comprises 102 sensor groups, each containing one magnetometer and two planar gradiometers. Before entering the shielded room, four head-position-indicator (HPI) coils were attached to the participant's head for continuous head position tracking. The positions of the coils and individual anatomical landmarks were digitized using a Polhemus Fastrak system (Polhemus Inc., VT, USA). MEG data were sampled at a rate of 1000 Hz with a frequency range of 0-330 Hz.

Eye tracking and gaze-based control

A MEG-compatible EyeLink 1000 Plus eye tracker (SR Research, Canada) was positioned below the screen, operating in monocular mode at a frame rate of 1000 Hz. It was used both for real-time control of the gaze-controlled game and for recording gaze coordinates for offline analysis. Each 5-minute game session was preceded by a standard 9-point calibration, performed using the built-in SR Research algorithm. Gaze-based control was implemented via the Resonance platform (Nuzhdin 2019). An online algorithm analyzed gaze coordinates within a 500 ms moving window to detect gaze dwells. A dwell was recorded when two conditions were met:

(a) The range of both X and Y coordinates did not exceed 120 pixels, corresponding to 1.56° of visual angle from the participant's position (equal to the closest distance between cell centers on the game board), and

(b) No previous dwell had been recorded within 600 ms of the new dwell.

These prolonged dwells functioned similarly to mouse clicks or touchscreen taps in the traditional Lines game, triggering specific events based on various game conditions (see game description below).

The eye-controlled game

To simulate the natural behavior of users interacting with a gaze-based system, the experiment had participants freely play a specially designed eye-controlled game, EyeLines, originally described by (Shishkin et al. 2016b) and modified for the purposes of this study. The game was designed to elicit two distinct types of gaze behavior, both involving dwells (500 ms or longer): intentional gaze use for making moves, and spontaneous oculomotor activity (including visual exploration of the game board and deliberation on future moves without active interaction). This setup enabled the collection of a sufficient number of both intentional and spontaneous dwells. The game rules and software were structured to ensure that a significant proportion of long dwells could be reliably classified as either intentional or spontaneous. The classification of dwells into these two categories, along with the comparison of corresponding gaze and MEG data, was conducted during offline data analysis.

The EyeLines game board, displayed on a white background rectangular area (413 × 330 mm, 16.6° × 13.3°), was projected onto the screen (Figure 1). As in (Shishkin et al. 2016b), the board consisted of 7×7 square grey cells with equal gaps between them (in contrast to the original Lines game, typically played on a 9×9 board with a slightly different visual layout; these changes were introduced by Shishkin et al. (2016) to enhance gaze-based control). The distance between the centers of adjacent cells was 1.6°. An additional single cell, used to confirm gaze-based selections, was placed to the left of the board in half of the games and to the right (as shown in Figure 1) in the other half of the games.

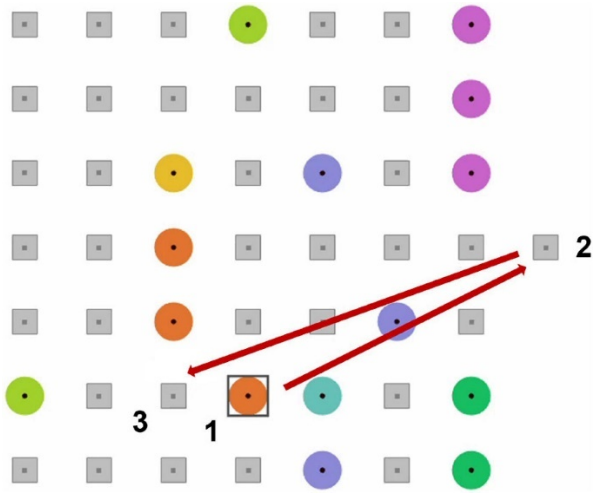

Figure 1. An example of *EyeLines* game position (Ovchinnikova et al., 2021, license CC BY). Here, a screenshot of an actual position is presented, with digits and arrows added to explain the sequence of gaze dwells required to make a move: 1 – dwell for selecting a “ball” (after 500 ms dwell, a square frame appeared around a ball), 2 – dwell on a remote “button” confirming the selection (after 500 ms dwell, a “ball” appeared over this cell), 3 – dwell on a free cell (after 500 ms dwell, the “ball” in cell 1 disappears and appears in cell 3). The distance between cell centers was 1.6°.

A participant's objective in the EyeLines game was to score as many points as possible. Points were awarded each time a participant successfully aligned four or more balls of the same color in a straight line. When such a line was formed, all balls within it disappeared from the board. After any other move, as well as at the start of each game, three colored "balls" appeared in randomly selected free cells on the board. Consequently, if a participant did not frequently create lines of four or more balls, the board would quickly fill up, leaving fewer available cells for new balls. The game concluded either when there were fewer than three free cells remaining, meaning no space for new balls, or after five minutes had elapsed without reaching this condition. At the end of the game, the participant’s score was displayed.

The color of each new ball on the board was randomly chosen from seven possible colors. A different color was used for the ball that appeared in the confirmation button position. To aid in fixation accuracy, black dots were placed at the centers of balls and empty cells.

As in the original Lines game, each move in EyeLines involved selecting a ball and then selecting a free cell to which it should be moved. Moves were only possible if a "free path" of adjacent free cells existed between the ball's initial and new positions. Unlike the original Lines game, in EyeLines, selections of both the ball and the new cell were made using gaze dwells (see above the Eye tracking and gaze-based control section for details). Ball selections had to be confirmed by fixating on a confirmatory "button," a cell located outside the board (labeled as position 2 in Figure 1; hereafter referred to as "the button," as this term was used to explain the move process to participants).

Participants were instructed to execute each move by following this sequence of actions:

(a) Identify the ball they wish to move and the free cell to which they intend to move it.
(b) Fixate on the ball until a square frame appears around it ("ball pre-selection," labeled as position 1 in Figure 1).
(c) Fixate on the button (position 2 in Figure 1) until a ball of a different color appears within it, indicating that the selection has been confirmed ("selection confirmation").
(d) Fixate on the free cell where the ball is to be moved (position 3 in Figure 1) until the ball is "moved" to it ("ball movement").

The "ball movement" process involved several simultaneous events: the selected ball and the frame around it disappeared from position 1, the ball indicating the selection disappeared from position 2, and the "moved" ball appeared in position 3, maintaining the same color as the ball originally in position 1.

All events—"ball pre-selection," "selection confirmation," and those comprising "ball movement"—were triggered by 500 ms dwells detected online, as explained in the previous subsection, under the additional condition that the median gaze coordinates within the 500 ms time window fell within a 120 x 120 pixel area (1.6 x 1.6°), centered on the related ball, button, or free cell. (Instead of two dwell time thresholds, 500 ms and 1000 ms, used by (Shishkin et al. 2016b), we only used only the shortest one, as it allowed for the collection of a sufficient number of intentional and spontaneous gaze dwells of similar duration).

Participants were instructed that if a frame appeared unexpectedly around a ball they did not intend to select, they should simply ignore it, as only the most recently pre-selected ball could be confirmed via a button dwell. They could change their pre-selected ball by dwelling for 500 ms on any other ball. In such cases, the frame would disappear from around the previously pre-selected ball and reappear around the newly pre-selected ball. There were no limitations on the number of selection changes.

In data analysis (described below), ball pre-selections followed by a dwell on another ball rather than a button dwell were categorized as spontaneous dwell. In contrast, quickly confirmed ball pre-selections were classified as intentional dwells. These details were not disclosed to participants; they were only informed that the purpose of the experiment was to study brain activity during gaze-based interaction with a computer.

The requirement of pre-selection confirmation via a button dwell differed from the game design used in (Shishkin et al. 2016b). In that study, a button dwell activated control, allowing immediate selection of a ball through subsequent dwells. Spontaneous dwells were defined as those occurring without prior activation of control. However, in that design, a high-amplitude saccade from the activation button preceded intentional dwells, introducing "contamination" from saccade-related brain and oculographic activity. Additionally, the amplitude of the preceding saccade strongly influences brain activity early in the course of fixation (e.g., (Nikolaev et al. 2016)). Therefore, the game design was modified to equalize, as much as possible, the onset conditions for intentionally and spontaneously prolonged fixations, minimizing the influence of factors unrelated to voluntary control.

Procedure

Participants received instructions and engaged in at least two practice games with the confirmation button positioned on both the left and right sides. Additional adjustments to the eye tracker, further instructions, and/or additional practice sessions were provided if necessary. Once the participant demonstrated adequate gaze-based control and a clear understanding of the game rules, the main series of eight games commenced. Eye tracker calibration was performed before each game, including the practice sessions. Participants were allowed a rest period of 1-3 minutes between games. The

experimenter continuously monitored the participant's gaze, which was displayed as a dot moving over a copy of the game board. If signs of poor control were observed (an infrequent occurrence, happening no more than once per participant), the game was halted, its data discarded, and a new calibration was conducted before restarting the game.

All eight games were played under identical conditions for all participants, with the only variable being the position of the confirmation button. The button's position for the first game was randomized and counterbalanced across participants. In subsequent games, the button position alternated between symmetrical left and right positions (Figure 1 provides an example of the right button position)..

Gaze data analysis

The primary focus of the analysis was on gaze dwells lasting longer than 500 ms on balls, which led to ball pre-selection during the game. Preprocessing of online-detected dwells involved the following steps:

(a) Rejection: Dwells longer than 500 ms were rejected if gaze coordinates were partially lost (e.g., due to blinks detected online by the SR Research algorithm, or eye tracker malfunctions) or if the participant violated instructions or game rules (e.g., dwell on a free cell without prior selection confirmation, or attempting to move a ball to a cell with no available path).

(b) Onset correction: The onset time of the dwell and the time of leaving the fixated object were corrected. This step involved identifying an eye fixation detected by the built-in eye tracker algorithm, which matched the > 500 ms dwell identified by the EyeLines algorithm (using criteria for saccades: acceleration > 8000˚/s², speed > 30˚/s, and a minimum duration of 6 ms). If no fixation was detected by the eye tracker within 50 ms of the EyeLines dwell onset, the latter was discarded (occurring in less than 5% of cases). Otherwise, the time of the closest fixation identified by the eye tracker was used as the corrected dwell onset. The dispersion-based algorithm was preferred for online interaction due to its perceived naturalness and effectiveness in pilot studies, while the built-in eye tracker criterion provided the precise moment of gaze stop, which was crucial for MEG data analysis. This procedure

effectively excluded most dwells with incorrectly defined onsets due to slow response times in the online interaction algorithm (e.g., calibration issues).

(c) Labelling: The identification of spontaneous and intentional dwells was primarily determined by subsequent events, such as dwell on another ball or the confirmation button. However, additional filtering of dwells associated with specific gaze behavior patterns was necessary to ensure a high level of certainty regarding strictly intentional dwells (i.e., those intended from the outset). The selection of dwells for analysis was based on the alignment between the eye movement pattern and the expected behavior of the player during spontaneous or intentional ball selection. Specifically, an intentional ball selection should be promptly confirmed by activating the button, ultimately leading to the execution of a move. To evaluate this, we analyzed the delay in the participant's response to feedback from the selected ball (the time from ball selection to the initiation of a saccade) and the time taken to shift gaze to the confirmation button (the time from the first saccade after selecting the ball to the onset of the dwell on the button). For most participants, the mode of the reaction time histogram fell within the range of 270-320 ms, while for others, it was shifted to approximately 400 ms explained by the more frequent occurrence of delayed reactions. To capture the most representative reaction time interval, a threshold of 500 ms was established for reaction speed to the ball's feedback to identify intentional dwells. For the time required to shift gaze to the button, a threshold of 200 ms was chosen, which exceeds the typical duration of a single saccade but is insufficient to allow for additional dwells that could indicate a search for a favorable spot for a spontaneously selected ball. The main criterion for identifying spontaneous selections was the presence of at least one unconfirmed selection of another ball. This ensured that the chosen dwell was not a result of calibration or activation issues, which could have led to a missed selection of the intended ball.

MEG preprocessing

Sensors with contaminated signals were manually excluded, and the MaxFilter routine (MEGIN/Elekta Oy, Helsinki, Finland) was applied using the following settings: temporal signal space separation (tSSS) (Taulu and Simola 2006) with t = 10 s and corr = 0.9, movement correction (MaxMove), and head origin

normalization to the standard position (for details, see MaxFilter User's Guide, https://ohba-analysis.github.io/osl-docs/downloads/maxfilter_user_guide.pdf).

Synchronization of MEG and eye tracker data was achieved for each game by adjusting the MEG time so that the synchronization triggers in both datasets coincided. MEG recordings were segmented into epochs of [-1000 2000] ms relative to the onset of spontaneous and intentional dwells. MEG analysis was divided into two pipelines aimed at investigating evoked power (phase-locked event-related fields) and induced power (non-phase-locked activity in the alpha and beta bands).

Induced power analysis

To explore the oscillatory dynamics during both spontaneous and intentional dwells, we employed the method of simultaneous diagonalization of covariance matrices of the signal in compared conditions (generalized eigendecomposion, GED – see also (Cohen 2022; Nordhausen and Ruiz-Gazen 2022; Parra and Sajda 2003)). This method enables the analysis of multidimensional data (in our case – MEG) by utilizing hypothesis-driven spatial filters to enhance distinctions in the power of signal frequency bands, while concurrently minimizing irrelevant activity and reducing data dimensionality. Our hypothesis posited distinct manifestations between intentional and spontaneous dwells, specifically focusing on variations in levels of disinhibition within the eye motor system (as indicated by central alpha(mu) and beta rhythms), and the divergent engagement of the visual analyzer (potentially, leading to alterations in occipital alpha). We anticipated intentional dwells to demonstrate controlled inhibition in eye movement, whereas spontaneous dwells were expected to engage in simultaneous visual information processing and saccadic activity.

Therefore, our investigation focused on combined alpha+beta frequency range (8–30 Hz) within the interval [-0.25 – 0.4] seconds relative to fixation onset, which encompassed the saccade and the primary phase of the dwell.

While individual analysis is typically more sensitive, it presents challenges for interpretation at the group level due to difficulties when matching corresponding components across individual participants. Therefore, for this analysis, we opted for a less sensitive method involving pooling signals from all

participants and the computation of group-level spatial filters (components). In accordance with the recommendations outlined in (Cohen 2022), the following algorithm was employed for analysis:

1) We equalized the number of participant's spontaneous and intentional epochs by randomly selecting a maximum of 100 epochs per condition and per participant. If there were less than 100 epochs per condition, we randomly selected from the condition with highest epoch number in a participant same number of epochs which was in the condition with lower number of epochs. As the result of this procedure, 20 participants had between 95-100 epochs per condition, while the remaining participants had between 50-80 epochs per condition, resulting in a total of 2560 epochs per condition for the whole group. No participant had less than 50 epochs per condition.
2) To reduce contribution of evoked components, MEG signals were averaged over epochs and subtracted from each epoch (this procedure was done separately for spontaneous and intentional epochs and for each participant). Epoch signals were normalized for each participant using the median absolute deviation (MAD) so that all gradiometers collectively and across all epochs [-2 – 2] s relative to fixation onset had MAD of 1 for that individual, while all magnetometers also had MAD equal to 1.
3) Signals were bandpass-filtered in 8-30 Hz frequency range using FIR zero-phase filter. Following that, dimensionality reduction of the data was performed using PCA retaining only components that explained at least 0.001% of the variance (resulting in a total of 77 components), ensuring that the data were full rank.
4) Covariance matrices were computed: one for each condition for all participants collectively (subsequently denoted as S for intentional trials and R for spontaneous trials) followed by generalized eigendecomposition (GED) computation expressed by the following formula:

Equation 1

$$\Lambda = \mathrm{argmax}\left\{\frac{\mathrm{W^T SW}}{\mathrm{W^T RW}}\right\}$$

Where Λ denotes the eigenvalues of the SR^{-1} matrix, the columns of W represent the spatial filters (inverse operators) for de-/synchronization components, and W^{-T} represents forward models of the components (Haufe et al. 2014).

5) To mitigate overfitting, step 4) was repeated 10,000 times with trials' label permutation. We retained columns of W whose eigenvalues exceeding the 1th percentile (for the first components) or the 99th percentile (for the last components) of the permutation distribution based on comparisons between the original Λ obtained and the distribution obtained through permutations.
6) For epochs projected onto the selected components, time-frequency wavelet transform was performed using the Morlet wavelet with a variable number of cycles following the procedure proposed by (Moca et al. 2021). Wavelet scales were linearly spaced from 3 to 45 Hz with 0.5 Hz step, minimum number of cycles was set to 5 with 1 to 30 superresolution order as described by Moca et al., power values were converted to decibel. Spectrograms were generated by averaging all trials with trimmed mean with 10% of marginal values removed, followed by either calculating difference between conditions, or baseline subtraction represented by mean value within [-1.5 – -1] s interval prior to fixation onset.
7) To evaluate the statistical significance of differences in synchronization levels among oscillatory components, we utilized differential spectrograms contrasting intentional and spontaneous conditions. Statistical significance was determined through a permutation cluster test. Namely, the differential spectrograms were computed for randomized partitioning into intentional and spontaneous trials, repeated 10,000 times; all differential spectrograms were converted into binary matrices, with a value of 1 assigned to data falling within the marginal 1% distributions derived from permutations and 0 for the rest of the data; a threshold for the size of the largest cluster (contiguous area of «1» pixels) was determined as the 99th percentile of encountered on permuted maps. Finally, these thresholds were applied to the differential spectrogram maps based on true label partitioning, defining statistically significant time-frequency clusters.

This procedure was also separately applied to alpha (8–15 Hz) and beta (15–30 Hz) ranges as well as pre- and post-onset time intervals ([-0.4 – 0], [0 – 0.4] seconds). In these cases, only shifts in statistical significance of spatial components and band power statistics were obtained, while the whole pattern of the results followed what was revealed in the broad band analysis. To save space, we do not report these results.

Evoked fields analysis

The multivariate approach of extracting significant spatial projections, which we employed in the analysis of induced activity, can also be used in the analysis of phase-locked, evoked signal components (Cohen 2022; de Cheveigné and Parra 2014). Two adaptations for evoked activity were proposed, denoising source separation (DSS) (Särelä et al. 2005)) and Fischer-criterion beamforming (FCB) (Pires et al. 2011). They were applied for multidimensional EEG and MEG analysis in a number of studies (Das et al. 2020; Molloy et al. 2019; Presacco et al. 2016). These methods are effectively a dimensionality reduction procedure with output components optimized according to two criteria: reducing within-condition variance (i.e., isolating phased-locked responses and suppressing non-phased-locked activity) while simultaneously increasing between-condition variance (i.e., differences between compared conditions). A small distinction between DSS and FCB lies in the fact that in DSS, the optimization steps for evoked activity and differences between conditions are separated, while FCB addresses them simultaneously.

We applied FCB to test the hypothesis that evoked activity differs between compared conditions: spontaneous and intentional gaze delays. Similar to the algorithm utilized for analyzing induced activity, the following algorithm was employed for evoked fields:

1) The same epochs were selected (2560 per condition) as for induced activity analysis (see step (1) in induced analysis).
2) Epochs underwent a 20 Hz low-pass filtering using FIR zero-phase filter, baseline correction to the interval [-0.3 – -0.1] s, and normalization to the overall standard deviation of the same baseline interval across all epochs within the same participant.

3) The Fischer-criterion beamformer was computed for the interval [0 – 0.4] s. Unlike for induced activity, the pre-fixation period was not considered to avoid signal contamination from saccadic artifacts. The Fischer criterion is solved as follows (Pires et al. 2011):

Equation 2

$$\Lambda = \text{argmax}\left\{\frac{\mathrm{W^T S}_b \mathrm{W}}{\mathrm{W^T S}_w \mathrm{W}}\right\}$$

Where Λ denotes the eigenvalues of the $S_b S_w^{-1}$ matrix, S_b represents the between-condition matrix, and S_w represents the within-condition matrix, computed from

Equation 3

$$S_b = \sum_i (\overline{X}_i - \overline{X})(\overline{X}_i - \overline{X})^T$$

Equation 4

$$S_w = \sum_i \sum_{k \in C_i} (X_{i,k} - \overline{X}_i)(X_{i,k} - \overline{X}_i)^T$$

where $i \in (Ci, Cs)$, with Ci denoting the intentional condition, Cs denoting the spontaneous condition, and $\overline{X}_i$ и $\overline{X}$ representing the arithmetic average across a condition or across all epochs.

4) Similar to induced field analysis, step 3) was repeated 10,000 times with trials' label permutation, retaining only components with Λ above the 99th percentile of the permutation distribution.

5) Epochs were projected onto the selected components and rescaled to the standard deviation of the baseline interval [-0.3 – -0.1] s as in step 2), and a 1% confidence interval was evaluated for differential ERF using permutation test (Efron and Tibshirani 1994). To achieve this, differential evoked fields, after using median averaging per condition and participant, were obtained with condition label permutation (10,000 times), their amplitude was thresholded with

a 1% threshold from the distribution, and continuous segments (time-clusters) above the threshold were filtered based on a 1% magnitude from the clusters observed for the recombinant distribution.

6) Selected components from step 4) were projected back onto the sensor space for source-level visualization, enabling a collective analysis irrespective of their amplitude while considering their mixing.

Source-level analysis

Due to unavailability of participants' MRI data, Colin27 brain template (Holmes et al. 1998) was used to compute cortical activation patterns. The cortical surface meshes comprised 10,000 vertices (sources) across both hemispheres. Statistical inference in this study was conducted on sensor-level data, however, employing source localization techniques could yield valuable insights into the specific brain regions underlying the observed evoked and induced dynamics.

Forward model computation was performed with Brainstorm (Tadel et al. 2011), which is documented and freely available for download online under the GNU general public license (http://neuroimage.usc.edu/brainstorm). The forward solution was calculated using overlapping spheres approach (Huang et al. 1999). The inverse solution was computed by Brainstorm built-in minimum norm estimation algorithm applied with the default settings ("kernel only" as the output mode, three as the signal-to-noise ratio, the source orientation constrained to perpendicular to the cortical surface, the depth weighting restricting source locations to the cortical surface and the whitening PCA). A noise covariance matrix, necessary to control noise effects on the solution (Bouhamidi and Jbilou 2007), was calculated either from empty room recording (induced analysis) or from baseline interval for (evoked analysis).

For both evoked and induced analyses, the group-level pattern (filter's forward model) of each significant component was multiplied by individual inverse operators, normalized for each participant (ensuring the sum of absolute values across all sources was set to 1), and subsequently averaged across participants in the source space. Sources located on the medial cortical surface, including the corpus

callosum and cingulate cortex, were excluded. Thresholded vertices—those with weights exceeding 50% of the maximum source magnitude (corresponding to the top 6.5% for induced components and 9–11% for evoked components)—were clustered to retain only spatially distinct activations, defined as clusters with more than 100 sources and inter-source distances of less than 1 cm. These activations were visualized on cortical surface meshes. To determine the anatomical locations of the components, the weighted centroids of source clusters were calculated in MNI-normalized space. To ensure accuracy, clusters were constrained to remain within a single hemisphere and limited to either the dorsal or ventral surface of the cortex. This approach prevented centroids from being positioned deep within or between hemispheres.

Control for eye movement artifact contribution

Eye movements can significantly differ between spontaneous and intentional dwells, and related artifacts are common in brain signals co-registered with eye tracker data (Nikolaev et al. 2016). In our evoked MEG data analysis, we employed a signal separation procedure that itself provided some level rejection of eye movement-related interference. However, synchronizing MEG data with eye movements may still increase the likelihood of eye movement artifacts contaminating the MEG signal, making it essential to verify the potential contribution of such artifacts to the observed MEG components. We selected trials preceded by a shift in either the OX or OY coordinates of plus or minus 200 pixels (i.e. right, left, up and down) within a 100 ms window around dwell onset (i.e., saccades with amplitudes larger than 2.6°). We then averaged their evoked fields and eye tracker data, visually inspecting the resulting plots for any signs of eye movement artifacts contributing to the evoked fields. For analysis of induced activity, spectrograms were examined for the presence of low-frequency dominated broadband activity, characteristic of blink and saccade artifacts. A secondary check, applicable to both induced and evoked components, involved inspecting the patterns (forward models of separating filters) for any contribution to the signal from the frontal sensors.

Results

Data labelling

On average, the game consisted of 36±7.6 moves (mean±SD), with an average time between moves of 8.28±1.78 seconds. Ball selections (including unconfirmed ones) occurred every 3.35±0.50 seconds. Detailed information for each participant can be found in Table S1. The labeling of dwells that led to ball selections, according to the criteria described in the Methods (see section Gaze Data Analysis), revealed a 2:5 imbalance in favor of spontaneous dwells. The total number of dwells that met all the eye-tracking data quality criteria was 12,023 across 29 participants. In the next step, dwells with abnormal MEG signals were excluded, and the number of spontaneous and intentional dwells was balanced for each participant, leaving a total of 6,748 dwells with a 1:1 ratio between spontaneous and intentional. For the MEG analysis, the number of dwells was further reduced to ensure equal contribution from each participant to the group analysis, resulting in a total of 5,120 dwells. For all subsets, the dwells corresponding to games with the button positioned on the right and left were balanced, with a 52:48 split for the whole sets. The number of dwells per participant in the raw data, at different stages of data pruning and in the final dataset is presented in Figure S1.

Gaze behavior

Labeling dwells as spontaneous and intentional was based on different gaze behavior patterns prior to and after the dwells (roughly illustrated in Figure 2A). Therefore, it was not unexpected that certain eye movement characteristics differed dramatically between intentional and spontaneous dwells. However, the distance of the gaze from the center of the dwell (median over the interval 0-500 ms; the left panel of Figure 2B) had almost identical time courses for intentional and spontaneous gaze dwells in the first 200-250 ms. The corrective saccade typically occurred at the same time (around 200 ms) and had similar amplitude in the two types of dwells. After 250 ms, in the case of intentional dwells, gaze movements were restricted to a small area (0.1°) around the center. In contrast, for spontaneous dwells, the gaze rapidly shifted away from the center; as we analyzed only cases where the gaze remained within the "sensitive" area of the ball until 500 ms, up to this time the deviation was moderate "by definition".

Change in distance to the ball's center (the right panel of Figure 2B) indicated that during intentional dwells, the gaze progressively moved closer to the center, whereas during spontaneous dwells, the gaze drifted away, likely due to attention shifting to surrounding elements of interest. Additionally, intentional dwells were characterized by a synchronous saccade around 750 ms, directed toward the confirmation button. This 750 ms point, i.e., about 250 ms after the onset of the visual feedback indicating ball selection, should correspond to time when participants were able to react to the feedback. As a result, dwell time (duration) distribution beyond the 500 ms threshold highly differed between intentional and spontaneous dwell (Figure 2C, left).

When examining the characteristics of the saccades preceding the dwell, only slight and statistically insignificant differences were observed between the conditions. There was a trend toward higher peak velocity ($p = 0.071$; Figure 2C, center) and amplitude ($p = 0.078$; Figure 2C, right) in the intentional condition, likely due to some pre-planned selections of distant balls.

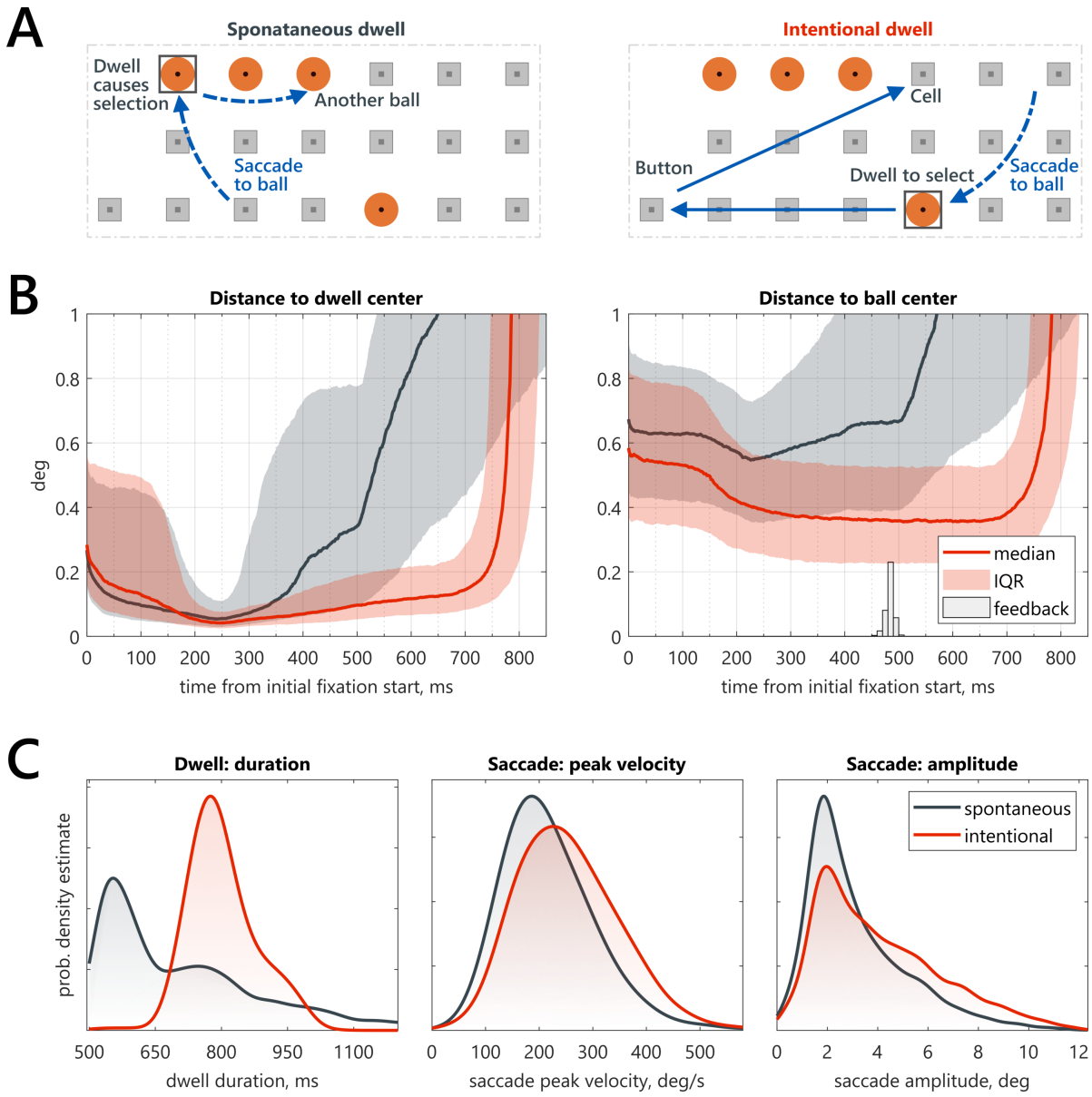

Figure 2. Characteristics of eye movement activity during spontaneous and intentional dwells. A – Schematic sequence of dwells and saccades during spontaneous (left) and intentional (right) ball selections. B – Average time courses of gaze deviation from the center of the dwell (left) and from the center of the target ball (right). Black indicates spontaneous dwells, and red indicates intentional dwells, n = 3374 per condition. The timing of feedback is illustrated as a histogram. C – Histograms showing the distributions of the following metrics (from left to right): total dwell duration before gaze shift, peak saccade velocity and saccade amplitude, for the saccades preceding the dwell (towards the ball). Black indicates spontaneous dwells, and red indicates intentional dwells, n = 3374 per condition.

MEG: Induced power

The permutation test applied to GED components revealed two significant spatial components ($p = 0.0034$ and $p = 0.0053$), which differentiated intentional and spontaneous dwells (their sensor-level topographies are shown in Figure 3, top panel). These components exhibited central localization, lacked left-right asymmetry, and were marked by pronounced event-related synchronization (ERS) within the alpha and beta ranges of MEG (Figure 3, bottom panel). This synchronization began approximately 0.75 seconds before the onset of fixation, intensified around the onset, and peaked approximately 0.25 seconds afterward.

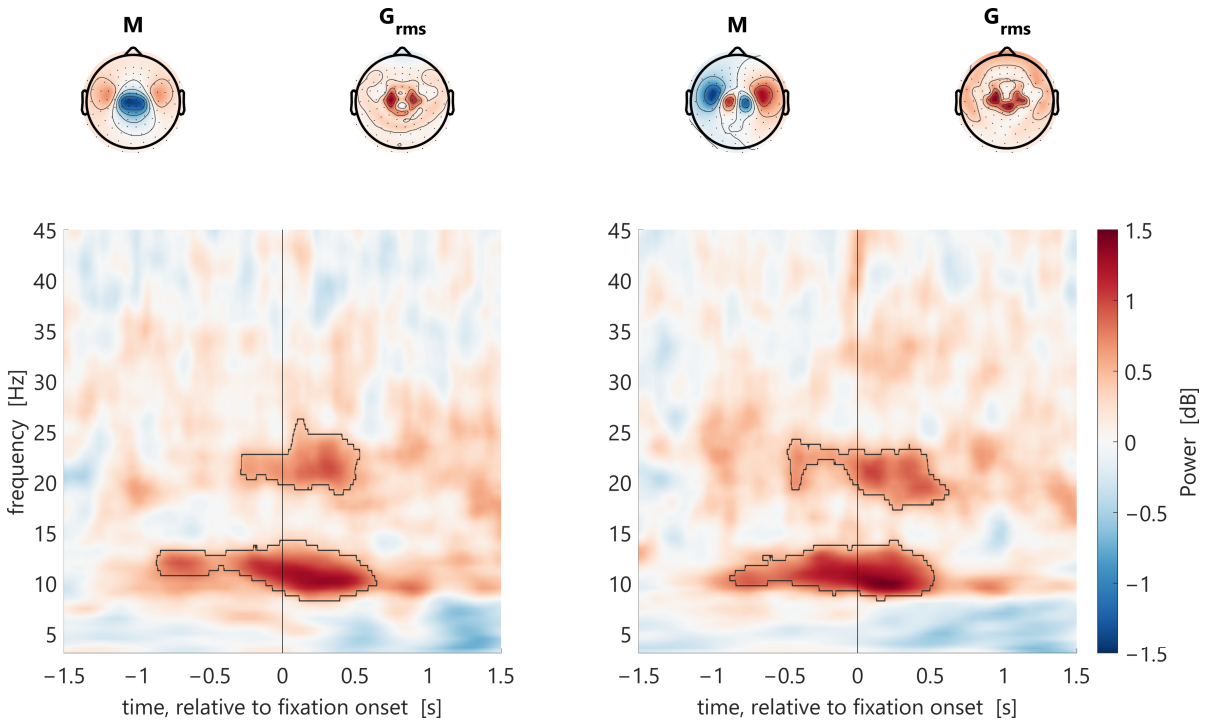

Figure 3. Differential oscillatory dynamics between intentional and spontaneous gaze dwells. Two statistically significant induced field components are presented in the left and right panels, respectively. The top section displays the forward models of components projected onto magnetometers (M) and the root mean square of planar gradiometers (G_{rms}). The bottom section presents time-frequency maps are shown, with statistically significant clusters outlined by solid black lines ($p < 0.01$).

Based on the dipole structure inferred from the components' forward models, it appeared that each component was generated by two closely positioned dipoles with different orientations (Figure 3, upper panel). Notably, the ERS diminished around the 0.5-second mark and did not persist for the entire dwell duration, which typically lasted around 750 milliseconds (Figure 2B).

The differences between conditions seem to result from two factors: event-related synchronization during intentional gaze dwells and a reduction or absence of desynchronization observed in spontaneous dwells (refer to the time-frequency plots in Figure S2). This suggests a shift in inhibition: spontaneous dwells are marked by disinhibition both before and during dwells, while intentional dwells coincide with an increase in inhibition, particularly during the early stages (0 – 300 ms) of gaze dwell. Note that creating accurately baselined maps poses a challenge due to the rapid succession of intentional and spontaneous gaze dwells in this free-behavior experiment, thus we applied statistical analysis only to the difference spectrograms. Significant clusters are denoted by solid black lines in the time-frequency plots (Figure 3, bottom).

Source-level analysis unveiled the localization of two primary components, which extensively overlapped. They were situated in both the motor and premotor cortex, consistently aligning with the frontal eye field (FEF) and supplementary eye field (SEF) areas (see Figure 4 and Table S2).

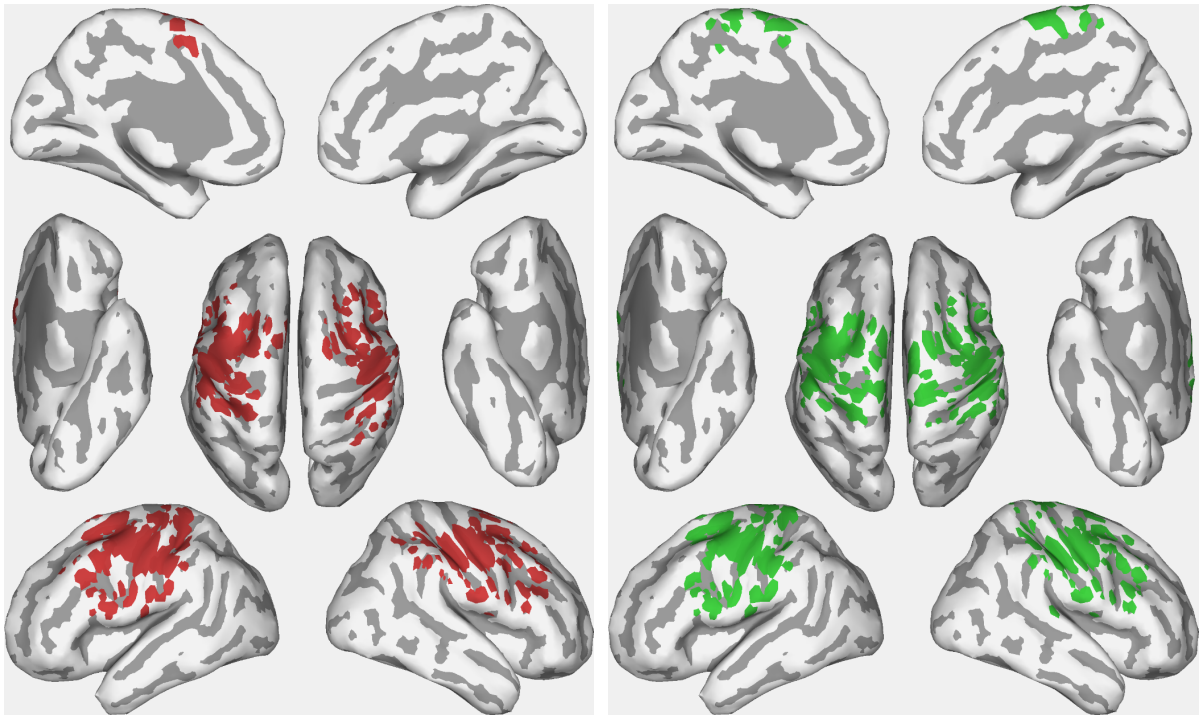

Figure 4. Source representation of two significant components for oscillatory alpha+beta range (8–30 Hz).

MEG: Evoked fields

Analysis using the Fischer criterion beamformer and subsequent eigenvalue significance testing revealed three significant components ($p<0.0001$, $p<0.0001$, $p=0.0096$, respectively) (Figure 5, Table S3). The first component, with the largest effect size, exhibited a pronounced deviation in the magnetic field under intentional condition, starting shortly (-100 ms) before fixation onset and persisting until the end of dwell as well as next intentional action (button activation). The second component was characterized by an initial positive deviation from -0.05 to 0.08 s under the intentional condition, followed by a negative deviation from 0.35 to 0.750 s. The third component showed negative and positive deviations within the interval from 0 to 0.05 s, followed by a negative deviation coinciding with the onset of the subsequent intentional confirmatory saccade (from 0.7 to 0.8 s).

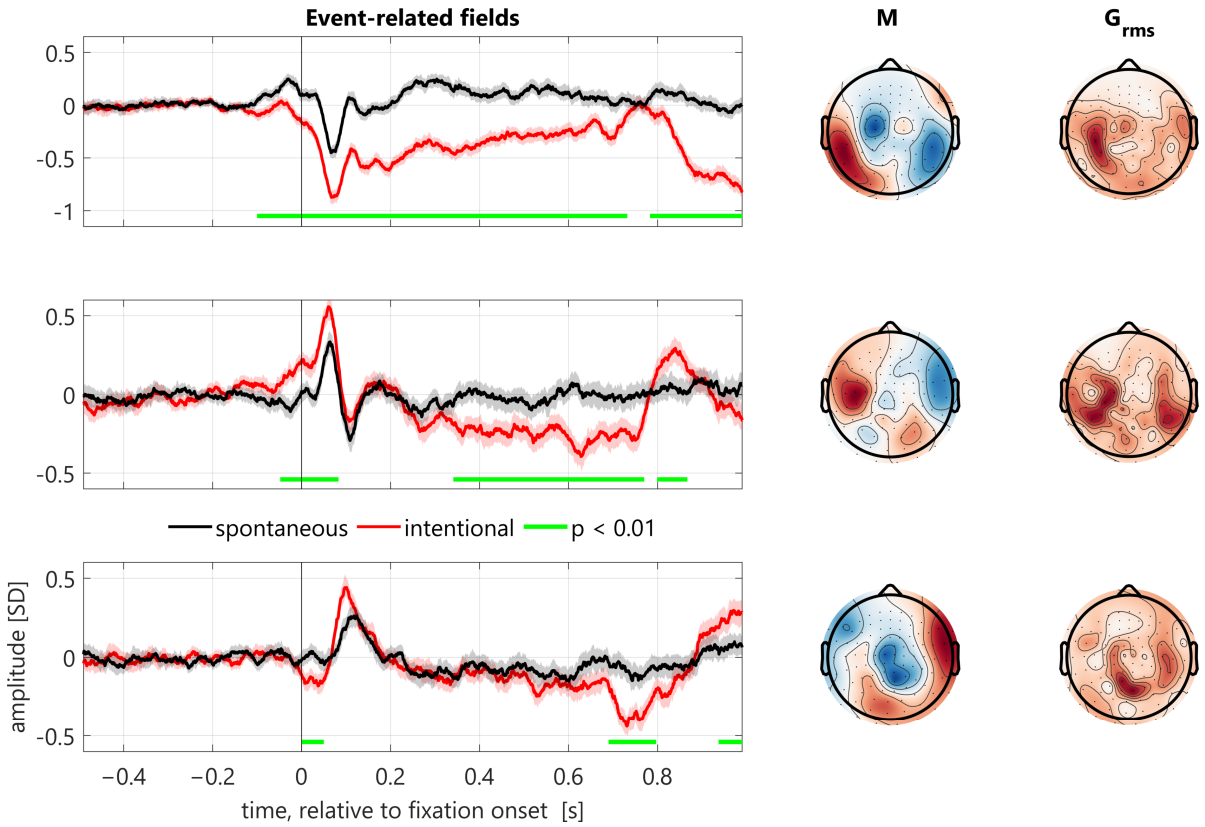

Figure 5. Event-related fields of the three significant spatial components. Left panel: average (median) time-courses of components with bootstrap confidence interval of the median shown as colored shade. Right panel: sensor-level maps for the weights of forward models of the components projected onto magnetometers (M), and the root mean square of planar gradiometers (G_{rms}).

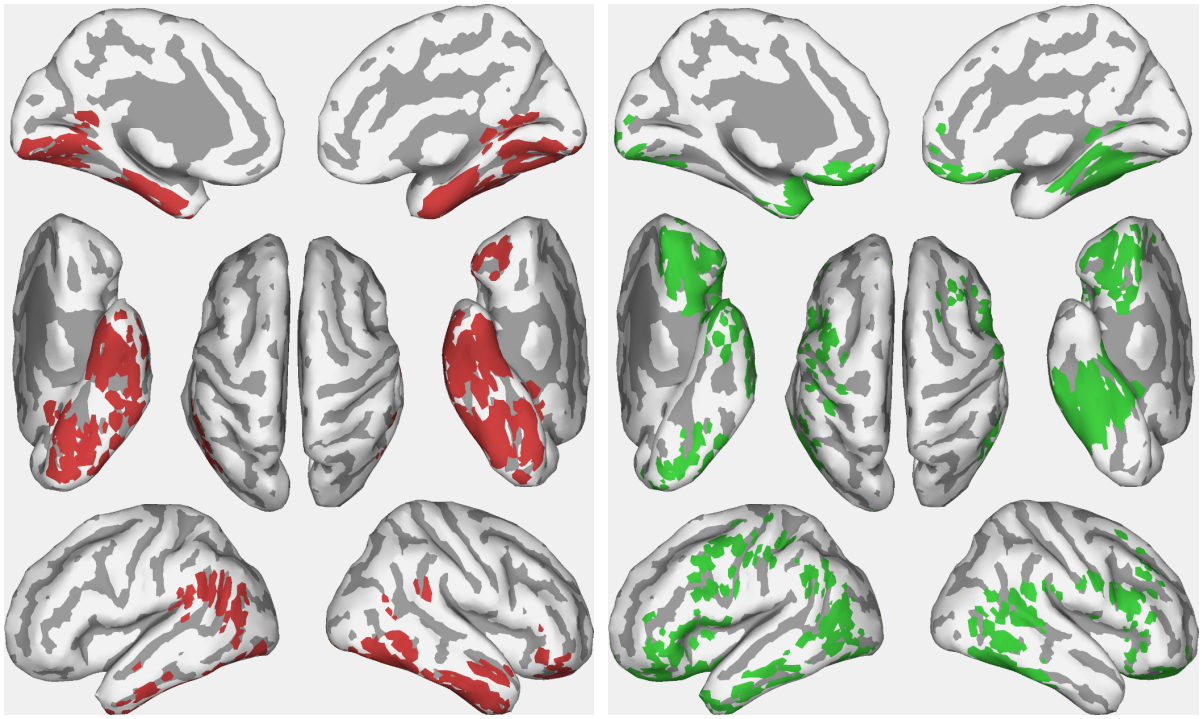

Figure 6. Source representation of the two significant spatial components for evoked fields (the earlier component is on the left, the later component is on the right).

Control for eye movement artifact contribution

We checked if the ERF data were significantly affected by eye movement artifacts by averaging trials where dwell onset was preceded by a saccade with an amplitude greater than 2.6° (corresponding to a 200 px change in gaze coordinates) along the OX axis (labeled 'right' and 'left'; Figure S3 and S4) and the OY axis (labeled 'up' and 'down'; Figure S5 and S6). In intentional trials, these saccades accounted for 40.3% (OX) and 35.1% (OY) of all trials, while in spontaneous trials, they represented 26.6% (OX) and 24.7% (OY). The figures revealed no evidence of evoked component behavior that could be attributed to eye movement artifacts. Although large saccades did influence the time course of evoked components (see left panels on Figures S3-S6), they did not affect the difference between intentional and spontaneous responses (see right panels on the figures). Moreover, differences in oculomotor activity between spontaneous and intentional dwells (see Figure 2) could not account for the differences

in MEG components, as they emerged after 300 ms—later than the development of MEG responses (see Figures 3 and 5).

Discussion

In this study, we, for the first time, utilized gaze-based human-computer interaction technology to examine the neural mechanisms that support the voluntary suppression of eye movements without external guidance.

Previous human neuroimaging studies on eye-movement suppression have employed external stop signals, either before target presentation (as in the antisaccade task (Munoz and Everling 2004)) or after target onset (as in the countermanding paradigm (Kornylo et al. 2003)). Instead, our participants issued a gaze-based selection command by deliberately sustaining an extended fixation on a self-selected location on the game board. Our paradigm isolates the voluntary suppression of eye movements, removing additional processes related to stop-signal processing, redirection of attention, or preparation for a subsequent goal-directed saccade. By contrasting intentional and spontaneous fixations of extended duration, we were able to directly assess distinct characteristics of oculomotor activity, fixation-evoked responses, and oscillatory neural activity that specifically emerge during intentional gaze dwelling. Importantly, this approach reveals how intentional gaze withholding, in contrast to spontaneous dwelling, involves both top-down attentional control mechanisms and concurrent suppression within the oculomotor circuitry responsible for eye-movement initiation and planning, supporting a sustained focus on a defined spatial location.

In a broader perspective, the proposed contrast of intentionally vs. spontaneously prolonged gazes can be considered as a model for studying voluntary control and intention formation in general. Spontaneous eye movements and dwells are almost exclusively out of conscious control, unlike behaviors based on skeletal or even mimic muscle activity, and therefore may serve as a perfect control for voluntarily and consciously controlled intentional gaze behaviors in cognitive neuroimaging studies.

Oculomotor behavior characterizing intentional dwells

At the level of oculomotor behavior, we observed a notable difference between intentional and spontaneously occurring gaze dwells. Although both types showed strong suppression of eye movements during the first 200 ms after fixation onset, spontaneous dwells subsequently exhibited gradual gaze drift away from the fixation center (Figure 2B). In contrast, intentional gaze drift remained confined to a small (< 0.2°) spatial locus around the fixation center. Since smooth changes in eye position during natural fixations are typically involuntary (Krauzlis et al. 2017), this difference may suggest an active cortical control mechanism during intentional gaze dwelling, possibly enhancing precision for point-and-select actions via gaze.This inhibitory control appears to anchor the eyes firmly on the selected target, counteracting ocular drift, reducing discrepancies between eye and target position, and potentially preventing shifts in covert visual attention to peripheral locations, which are often accompanied by microsaccades and slower ocular drifts (Hafed and Clark 2002). This mechanism likely supports the precision and stability necessary for intentional gaze-stopping actions. The coupling of oculomotor behavior with MEG recordings in our study offers some insights into the neural underpinnings of this control system. (Note, however, that oculomotor inhibition is observed when a target is anticipated (Amit et al. 2019), and we cannot rule out that anticipation of a visual feedback from the gaze-sensitive interface could have similar effect).

Based on the observations made in this study, a separate line of research has been already started, where the *EyeLines* paradigm was used to extract intention-related features of oculomotor activity which differentiated intentional and spontaneous gaze dwells (Shevtsova et al. submitted; Shevtsova et al. 2023). A machine learning algorithm applied to these features made possible their online classification, so that participants could play the game effectively without making additional actions for intent labeling, such as selection confirmation or swithcing on the gaze-based control (Shevtsova et al., submitted).

Neural concomitants of intentional dwells

Research on humans and other primates suggests that suppressing spontaneous oculomotor behaviors relies on proactive inhibition within the frontoparietal saccade network (Johnston et al. 2019). The specific properties of cortical oscillations associated with intentional versus spontaneous gaze dwellings in our study (Figure 3, 4) align well with the functional inhibition of frontal cortical centers responsible for eye movement initiation and planning.

Firstly, we observed increased alpha and beta power during intentional vs spontaneous dwellings (Figure 3, 4), which likely indicated functional inhibition in the underlying cortical circuitry. In human EEG and MEG studies, alpha power increases across different task contexts are commonly considered a marker of selective inhibition in cortical areas involved e.g., (Jensen and Mazaheri 2010; Rihs et al. 2007), including those associated with eye movement planning and execution (Hwang et al. 2014). Supporting this, animal studies indicate that higher alpha power correlates with reduced neuronal firing—a hallmark of functional inhibition (Haegens et al. 2011).

Secondly, the topography of the differential alpha-beta band power increase was mainly bound to central scalp regions (Figure 3), suggesting a focus on motor rather than perceptual suppression. Source localization (Figure 4) confirmed that this oscillatory activity encompassed sensorimotor, premotor, and dorsolateral prefrontal cortex (DLPFC) regions, particularly including the frontal eye field (FEF) within the dorsal premotor cortex (at the junction of the superior precentral sulcus and superior frontal sulcus) and the supplementary eye field (SEF) along the border between medial and lateral surfaces of the frontal cortex (Figure 4, the first and the second components respectively). Research in nonhuman primates and human imaging studies suggests that SEF and FEF both contribute to ocular decision-making and the initiation of visually guided behaviors (Yang and Heinen 2014). Therefore, the 'functional inhibition' observed in these regions during intentional dwellings—evident in alpha and beta synchronization—may help establish a "status quo" state for the oculomotor system (see (Engel and Fries 2010)), potentially suppressing any shifts in gaze position.

Additionally, the relatively widespread alpha-beta increase we found in the frontal cortex during intentional gaze dwellings may arise from functional inhibition within a broader network of premotor and prefrontal cortical areas that contributes to the quieting of head and body movement, helping to keep the gaze within the designated spatial locus by minimizing disruptive head movements (Corneil et al. 2008). Notably, we did not observe significant intention-related modulations in the posterior cortical areas, specifically in the posterior cortical eye fields situated near the inferior parietal sulcus (IPS) that are involved in oculomotor behavior (Andersen 1989). This suggests that the oculomotor processes supported by the IPS may have been equivalent between spontaneous and intentional gaze dwells.

Thirdly, the timing of induced alpha-beta synchronization during intentional gaze dwellings implied that this oscillatory activity began at least a couple of hundred milliseconds before gaze stabilization within the intended spatial locus (Figure 3, Figure S2), suggesting a proactive inhibition control of the cortical saccade initiation network.

The latter finding is generally consistent with previous literature, though prior neuroimaging research has primarily focused on the preparatory period of the tasks requiring suppression of the prepotent oculomotor response upon the external cue (see, e.g., (Brown et al. 2006)). In the anti-saccade (AS) task, participants are instructed either to direct their gaze toward an upcoming visual target or to suppress this reflexive response and instead shift their gaze voluntarily to the opposite location, depending on the cue provided. Although human EEG/MEG research on the preparatory phase of the AS task remains limited, recent MEG findings indicate that successful task performance is associated with increased preparatory alpha-band power in the frontal eye fields (FEF) following the cue and prior to target onset (Hwang et al. 2014; 2016). Remarkably, a similar task-dependent increase in alpha oscillations was observed in monkey FEF local field potentials during a preparatory period when the monkeys were cued to inhibit a prepotent oculomotor response (Johnston et al. 2019). In this task, the monkeys had to either direct their gaze toward a large, high-luminance stimulus or inhibit this response in favor of a saccade toward a smaller, low-luminance stimulus. When instructed to suppress a reflexive gaze shift, prominent pre-stimulus alpha-band activity appeared in deeper FEF layers, correlating with

reduced neuronal firing in upper layers, suggesting that alpha-band rhythms in deep layers support proactive saccade inhibition.

Our results confirm and extend the previous literature, by showing that alpha-beta activity in the FEF and SEF, reflecting proactive, top-down inhibitory control, can arise without an external cue, solely driven by the intention to sustain gaze dwelling.

Alongside the induced oscillations, we observed distinctive evoked activity associated with intentional gaze withholding versus spontaneous gaze dwelling. The primary difference between these conditions in the fixation-onset-locked magnetic fields was not in transient ERF peaks but rather in a gradual DC shift in the evoked response waveform (Figure 5), suggesting sustained cortical activation associated with intentional gaze withholding. Literature suggests that such long-lasting evoked activation—extending from hundreds of milliseconds to several seconds in EEG/MEG—often emerges gradually in anticipation of predictable or relevant events and may be linked to attentional processing ((Pulvermüller and Grisoni 2020); for review see (León-Cabrera et al. 2024)). In our study, intentional fixations were indeed associated with the anticipation of the feedback from the gaze-sensitive interface, which allowed participants to terminate gaze holding and shift their gaze to another location (see Methods). However, the timing of the slow deflection, which peaked approximately 200-300 ms prior to, rather than at, the anticipated event, suggests it does not reflect preparatory cortical activity (Kononowicz and Penney 2016).

An alternative interpretation of the sustained neural activation evoked by intentional fixation is that it is attention-related. To use their gaze as a selection gesture, our participants needed not only to inhibit oculomotor behavior but also to concentrate and continuously focus on a self-selected spatial location on the game board. This steady focus was essential to effectively transmit a command to the computer, because it ensured that the gaze was kept in the “gaze-sensitive” area.

We propose that the sustained neural activation observed during intentional gaze dwelling reflects this voluntary spatial attention focusing on a specific spot. Based on its scalp distribution (Figure 5) and crude source localization (Figure 6), the cortical sources of this activity are primarily located in the

inferior convexity of the cortex, specifically in the posterior inferior temporal cortex (ITC) and inferior frontal regions (see also Table S3 for components 1 and 2).

Recent neurophysiological studies provide evidence that persistent neuronal firing in the posterior ITC is strongly modulated by spatial attention. The researchers emphasized that the posterior ITC may function as a distinct system for spatial attention focus, directing it according to an individual's internal objectives, thereby supporting cognitive programs relevant to goal-directed actions (Ramezanpour and Fallah 2022; Sani et al. 2021; Stemmann and Freiwald 2019). This system is thought to encode a "priority map" that determines which locations in the visual field are attended (Stemmann and Freiwald 2019). Intentional fixations in our study may thus recruit this spatial attention system to sustain gaze on a specific point, reducing diversions from that location.

The sustained activation of the orbitofrontal cortex (OFC)/ventral prefrontal cortex (PFC) (Figure 6) aligns with the proposed role of goal-directed spatial attention in intentional gaze fixations. In both primate neurophysiology and human neuroimaging studies, this region is recognized as part of the neural circuitry involved in oculomotor control, particularly in maintaining goal-relevant information (Fielding et al. 2015; Xu et al. 2017). During intentional gaze fixation, sustained OFC/ventral PFC activity may facilitate the registration of the intention to inhibit gaze shifts, potentially interacting with the ventral temporal attentional system to exert inhibitory control over eye movements.

Overall, our results neurophysiological suggest distinct functional roles for sustained evoked activation and induced oscillations during intentional gaze fixations, which were used to trigger a selection operation in the context of interaction with a computer. The prolonged evoked activation in the posterior inferior temporal cortex (ITC) and ventral prefrontal cortex (PFC), time-locked to fixation onset, appears to reflect the robust control of spatial attention on a specific location, thereby supporting the suppression of oculomotor behavior. Meanwhile, alpha-beta band oscillatory activity in the frontal eye fields reflects the strength and efficacy of this inhibitory control.

Limitations

Our study has several limitations. First, the precise timing of intention formation to select a specific spatial location on the game board could not be determined. While our results suggest that intention formation may be extended, encompassing both pre- and post-onset intervals, its timing likely varies across trials, potentially smearing the observed temporal patterns. Second, in our experiment design intentional dwells were different from the spontaneous ones not only by different degree of intentionality but also by different eye movement characteristics in the latter portion of the dwell and especially immediately after it, and by the presence of planned action to make a saccade to the confirmation location. It seems highly unlikely that these differences could affect our results, but they may restrict possible areas of the application of the proposed methodology. However, at least the issue of the saccade planning in case of intentional dwells can be solved by using more advanced gaze-based control techniques not requiring confirmation or similar actions, such as gaze-based control enhanced by machine learning and context-based predictions (Shevtsova et al. submitted; Shevtsova et al. 2023). Third, the absence of individual MRI data required us to use a standardized brain template, which may have introduced inaccuracies in localization. Fourth, performing the GED analysis at the group level rather than individually might have similarly affected the precision of our results. Despite these limitations, we believe they do not substantially impact the main findings of this study.

Intentionally prolonged gaze in natural behavior

The presented methodology of contrasting intentional and spontaneous gaze behavior observed in the context of using gaze-based interaction technology can be considered as being closer to the natural use of gaze than the experimental paradigms requiring significant efforts to modify reflective behavior.

More specifically, the origin of the ability to use gaze voluntarily may be related to its use in social interaction, where it is typically used without significant effort. Gaze-based social interaction is increasingly studied in behavior patterns like direct gaze (Adams and Kleck 2005; Hamilton 2016; Senju and Hasegawa 2005) and joint attention (Chevalier et al. 2020; Siposova and Carpenter 2019;

Tomasello and Farrar 1986). However, the main focus of such studies is often on gaze perception, and research on the active, "sending" side of gaze-based social interaction has only recently begun (Fedorova et al. 2015; Gobel et al. 2015; Hessels et al. 2019; Jarick and Bencic 2019; Riechelmann et al. 2021; Risko et al. 2016). In a more effortful task of avoiding one's partner's gaze the cortical activation pattern was similar to that observed in antisaccade tasks (Cavallo et al. 2015). To our knowledge, brain activity has not been yet studied in such social paradigms where gaze is under low-effort voluntary control. Such studies could likely bring new insights into voluntary gaze control, but gaze-based interaction with technical devices has some advantages as an experimental paradigm, as providing more strict control over the factors involved in an experiment.

Prospective application in hybrid eye-brain-computer interfaces (EBCIs)

It was suggested that on-the-fly estimation of the intentionality of a gaze dwell using the EEG can boost gaze-based interaction by preventing unwanted interface responses to spontaneous fixations/dwells, and even lead to creation of an especially fluent interaction between the user and a computer (Ihme and Zander 2011; Protzak et al. 2013; Shishkin et al. 2016b). To differentiate such a hybrid system from more mechanically combined BCIs and gaze interfaces, the term "eye-brain-computer interface" (EBCI) was proposed by Shishkin et al. (2016b). These studies focused on using, as a marker of intentionality, the expectancy wave (E-wave), also referred to as stimulus-preceding negativity (SPN) or non-motor contingent negative variation (CNV). Indeed, this EEG component was repeatedly found in intentional but not spontaneous gaze dwells in different paradigms: in the EyeLines game (Shishkin et al. 2016b), in a task involving selection of moving targets with smooth pursuit eye movement ("dynamical dwells") (Zhao et al. 2021), in target selection in extended reality (XR) (Reddy et al. 2024). Nuzhdin et al. (2017) demonstrated that a passive BCI using this "marker" could classify intentional and spontaneous gaze dwells non-randomly in online (near real-time) mode.

However, online performance of such a EBCI was found to be insufficient for practical application (Nuzhdin et al. 2017). One possible reason for this could be that E-wave is not specific to intentional gaze dwells but rather reflects the expectation of a confirmation signal from a gaze-sensitive interface,

which can occur even in the absence of an intention to interact with a computer. In one study (Shishkin et al. 2016a) classification of intentional and spontaneous dwells was improved using features of oscillatory EEG components, which could be, in principle, more specific to intentional gaze dwells. These results, however, could be biased because of possible contamination of the features by the saccade-related activity in the early part of the studied EEG interval, where a large saccade typically occurred due to specific organization of the experimental design; this possible contamination could not be reliably assessed, as no explicit spatial filtering was used.

In the current study we used a slightly different paradigm and a different intention labeling approach, providing clearer data at the dwell onset and better separation of intentional and spontaneous dwells. We also used MEG signals, which provide distinct information and enables better separation of spatial sources. We indeed found more detailed, previously unreported differences between spontaneous and intentional gaze dwells. Surprisingly, none of the differential MEG components exhibited the temporal profile characteristic of the EEG phase-locked marker for intentional dwells, namely a steady increase in amplitude culminating at the time point when confirmation gaze-interface feedback was expected. This discrepancy may be due to differences in how this activity is represented in MEG signals compared to EEG, with certain features being less pronounced in one recording modality than the other.

Earlier, feature-agnostic deep neural network algorithms to the MEG data effectively classified spontaneous and intentional dwell (Ovchinnikova et al. 2021). The findings of the current study provide a foundation for advancing this approach by identifying specific evoked and induced MEG signal components that could be targeted for on-line classification.

While conventional MEG systems are not well suited for human-machine interaction technologies due to their bulkiness and high cost, recent advancements of optically-pumped magnetometers (OPMs) (Boto et al. 2018; Boto et al. 2017) and continuing development of other types of compact, room-temperature sensors for human MEG (Koshev et al. 2021; Petrenko et al. 2021) have opened a perspective for MEG-based BCI applications (Bu et al. 2023; Iivanainen et al. 2023; Ji et al. 2024). In our view, these developments create the potential for MEG-based detection of intentional gaze dwells

to be incorporated into practical assistive technologies. Additionally, it may be valuable to explore EEG components corresponding to the MEG components identified in this study, with the goal of developing similar applications using EEG systems, which are more portable and cost-effective.

Implications for control conditions in neuroimaging

Maintaining gaze at a fixation cross or other small object is a commonly used "default" condition in neuroimaging studies. While our design required participants to fixate for a much shorter time than is typical in such studies, we observed that even this relatively modest demand elicited distinct activity across brain regions. This suggests that longer voluntary fixations could induce even more pronounced neural changes, as they may require greater effort. However, it is also possible that longer fixations might produce smaller effects, as some of the neural activity observed in our study may be transient in nature. Nonetheless, it seems likely that at least a portion of this activity would persist over time. Our study thus adds to concerns sometimes expressed in the literature (e.g., (Northoff et al. 2010)) that the fixation cross condition is not fully neutral and that its use as a standard baseline may lead to a certain bias. Additional studies should address this issue.

Acknowledgments

Authors thank A.O. Prokofyev and A.S. Yashin for their help in running experiments and MEG data preprocessing.

This work was supported by the Russian Science Foundation (grant number 22-19-00528).

The study was conducted at the unique research facility "Center for Neurocognitive Research (MEG-Center)" of MSUPE.

References

Adams RB, Jr., Kleck RE. 2005. Effects of direct and averted gaze on the perception of facially communicated emotion. Emotion. 5(1):3-11.

Amit R, Abeles D, Carrasco M, Yuval-Greenberg S. 2019. Oculomotor inhibition reflects temporal expectations. Neuroimage. 184:279-292.

Andersen RA. 1989. Visual and eye movement functions of the posterior parietal cortex. Annu Rev Neurosci. 12:377-403.

Boto E, Holmes N, Leggett J, Roberts G, Shah V, Meyer SS, Muñoz LD, Mullinger KJ, Tierney TM, Bestmann S et al. 2018. Moving magnetoencephalography towards real-world applications with a wearable system. Nature. 555(7698):657-661.

Boto E, Meyer SS, Shah V, Alem O, Knappe S, Kruger P, Fromhold TM, Lim M, Glover PM, Morris PG et al. 2017. A new generation of magnetoencephalography: Room temperature measurements using optically-pumped magnetometers. Neuroimage. 149:404-414.

Bouhamidi A, Jbilou K. 2007. Sylvester tikhonov-regularization methods in image restoration. Journal of Computational and Applied Mathematics. 206(1):86-98.

Brown MR, Goltz HC, Vilis T, Ford KA, Everling S. 2006. Inhibition and generation of saccades: Rapid event-related fmri of prosaccades, antisaccades, and nogo trials. Neuroimage. 33(2):644-659.

Brown MR, Vilis T, Everling S. 2008. Isolation of saccade inhibition processes: Rapid event-related fmri of saccades and nogo trials. Neuroimage. 39(2):793-804.

Bu Y, Harrington DL, Lee RR, Shen Q, Angeles-Quinto A, Ji Z, Hansen H, Hernandez-Lucas J, Baumgartner J, Song T et al. 2023. Magnetoencephalogram-based brain-computer interface for hand-gesture decoding using deep learning. Cereb Cortex. 33(14):8942-8955.

Cavallo A, Lungu O, Becchio C, Ansuini C, Rustichini A, Fadiga L. 2015. When gaze opens the channel for communication: Integrative role of ifg and mpfc. Neuroimage. 119:63-69.

Chevalier P, Kompatsiari K, Ciardo F, Wykowska A. 2020. Examining joint attention with the use of humanoid robots-a new approach to study fundamental mechanisms of social cognition. Psychon Bull Rev. 27(2):217-236.

Cohen MX. 2022. A tutorial on generalized eigendecomposition for denoising, contrast enhancement, and dimension reduction in multichannel electrophysiology. Neuroimage. 247:118809.

Corneil BD, Munoz DP, Chapman BB, Admans T, Cushing SL. 2008. Neuromuscular consequences of reflexive covert orienting. Nat Neurosci. 11(1):13-15.

Das N, Vanthornhout J, Francart T, Bertrand A. 2020. Stimulus-aware spatial filtering for single-trial neural response and temporal response function estimation in high-density eeg with applications in auditory research. Neuroimage. 204:116211.

de Cheveigné A, Parra LC. 2014. Joint decorrelation, a versatile tool for multichannel data analysis. Neuroimage. 98:487-505.

Duchowski AT. 2018. Gaze-based interaction: A 30 year retrospective. Computers & Graphics. 73:59-69.

Efron B, Tibshirani RJ. 1994. An introduction to the bootstrap. Chapman and Hall/CRC.

Engel AK, Fries P. 2010. Beta-band oscillations--signalling the status quo? Curr Opin Neurobiol. 20(2):156-165.

Ettinger U, Ffytche DH, Kumari V, Kathmann N, Reuter B, Zelaya F, Williams SC. 2008. Decomposing the neural correlates of antisaccade eye movements using event-related fmri. Cereb Cortex. 18(5):1148-1159.

Fedorova AA, Shishkin SL, Nuzhdin YO, Velichkovsky BM. 2015. Gaze based robot control: The communicative approach. 2015 7th International IEEE/EMBS Conference on Neural Engineering (NER); 2015: IEEE.

Fielding J, Clough M, Beh S, Millist L, Sears D, Frohman AN, Lizak N, Lim J, Kolbe S, Rennaker RL, 2nd et al. 2015. Ocular motor signatures of cognitive dysfunction in multiple sclerosis. Nat Rev Neurol. 11(11):637-645.

Funahashi S, Chafee MV, Goldman-Rakic PS. 1993. Prefrontal neuronal activity in rhesus monkeys performing a delayed anti-saccade task. Nature. 365(6448):753-756.

Gobel MS, Kim HS, Richardson DC. 2015. The dual function of social gaze. Cognition. 136:359-364.

Haegens S, Nácher V, Luna R, Romo R, Jensen O. 2011. A-oscillations in the monkey sensorimotor network influence discrimination performance by rhythmical inhibition of neuronal spiking. Proc Natl Acad Sci U S A. 108(48):19377-19382.

Hafed ZM, Clark JJ. 2002. Microsaccades as an overt measure of covert attention shifts. Vision Research. 42(22):2533-2545.

Hallett PE. 1978. Primary and secondary saccades to goals defined by instructions. Vision Res. 18(10):1279-1296.

Hamilton AFdC. 2016. Gazing at me: The importance of social meaning in understanding direct-gaze cues. Philos Trans R Soc Lond B Biol Sci. 371(1686):20150080.

Haufe S, Meinecke F, Görgen K, Dähne S, Haynes JD, Blankertz B, Bießmann F. 2014. On the interpretation of weight vectors of linear models in multivariate neuroimaging. Neuroimage. 87:96-110.

Hessels RS, Holleman GA, Kingstone A, Hooge ITC, Kemner C. 2019. Gaze allocation in face-to-face communication is affected primarily by task structure and social context, not stimulus-driven factors. Cognition. 184:28-43.

Holmes CJ, Hoge R, Collins L, Woods R, Toga AW, Evans AC. 1998. Enhancement of mr images using registration for signal averaging. J Comput Assist Tomogr. 22(2):324-333.

Huang MX, Mosher JC, Leahy RM. 1999. A sensor-weighted overlapping-sphere head model and exhaustive head model comparison for meg. Phys Med Biol. 44(2):423-440.

Hwang K, Ghuman AS, Manoach DS, Jones SR, Luna B. 2014. Cortical neurodynamics of inhibitory control. J Neurosci. 34(29):9551-9561.

Hwang K, Ghuman AS, Manoach DS, Jones SR, Luna B. 2016. Frontal preparatory neural oscillations associated with cognitive control: A developmental study comparing young adults and adolescents. Neuroimage. 136:139-148.

Ihme K, Zander TO. 2011. What you expect is what you get? Potential use of contingent negative variation for passive bci systems in gaze-based hci. International Conference on Affective Computing and Intelligent Interaction; 2011: Springer.

Iivanainen J, Carter TR, Trumbo MCS, McKay J, Taulu S, Wang J, Stephen JM, Schwindt PDD, Borna A. 2023. Single-trial classification of evoked responses to auditory tones using opm- and squid-meg. J Neural Eng. 20(5).

Isoda M, Hikosaka O. 2007. Switching from automatic to controlled action by monkey medial frontal cortex. Nat Neurosci. 10(2):240-248.

Jacob RJ. 1990. What you look at is what you get: Eye movement-based interaction techniques. Proceedings of the SIGCHI conference on Human factors in computing systems; 1990.

Jarick M, Bencic R. 2019. Eye contact is a two-way street: Arousal is elicited by the sending and receiving of eye gaze information. Front Psychol. 10:1262.

Jarvstad A, Gilchrist ID. 2019. Cognitive control of saccadic selection and inhibition from within the core cortical saccadic network. J Neurosci. 39(13):2497-2508.

Jensen O, Mazaheri A. 2010. Shaping functional architecture by oscillatory alpha activity: Gating by inhibition. Front Hum Neurosci. 4:186.

Ji D, Xiao X, Wu J, He X, Zhang G, Guo R, Liu M, Xu M, Lin Q, Jung TP, Ming D. 2024. A user-friendly visual brain-computer interface based on high-frequency steady-state visual evoked fields recorded by opm-meg. J Neural Eng. 21(3).

Johnston K, Ma L, Schaeffer L, Everling S. 2019. Alpha oscillations modulate preparatory activity in marmoset area 8ad. J Neurosci. 39(10):1855-1866.

Kononowicz TW, Penney TB. 2016. The contingent negative variation (cnv): Timing isn't everything. Current Opinion in Behavioral Sciences. 8:231-237.

Kornylo K, Dill N, Saenz M, Krauzlis RJ. 2003. Cancelling of pursuit and saccadic eye movements in humans and monkeys. J Neurophysiol. 89(6):2984-2999.

Koshev N, Butorina A, Skidchenko E, Kuzmichev A, Ossadtchi A, Ostras M, Fedorov M, Vetoshko P. 2021. Evolution of meg: A first meg-feasible fluxgate magnetometer. Hum Brain Mapp. 42(15):4844-4856.

Krauzlis RJ, Goffart L, Hafed ZM. 2017. Neuronal control of fixation and fixational eye movements. Philos Trans R Soc Lond B Biol Sci. 372(1718).

León-Cabrera P, Hjortdal A, Berthelsen SG, Rodríguez-Fornells A, Roll M. 2024. Neurophysiological signatures of prediction in language: A critical review of anticipatory negativities. Neurosci Biobehav Rev. 160:105624.

Majaranta P. 2011. Gaze interaction and applications of eye tracking: Advances in assistive technologies: Advances in assistive technologies. iGi Global.

Majaranta P, Bulling A. 2014. Eye tracking and eye-based human–computer interaction. Advances in physiological computing. Springer. p. 39-65.

Moca VV, Bârzan H, Nagy-Dăbâcan A, Mureșan RC. 2021. Time-frequency super-resolution with superlets. Nature communications. 12(1):337.

Molloy K, Lavie N, Chait M. 2019. Auditory figure-ground segregation is impaired by high visual load. Journal of Neuroscience. 39(9):1699-1708.

Munoz DP, Everling S. 2004. Look away: The anti-saccade task and the voluntary control of eye movement. Nat Rev Neurosci. 5(3):218-228.

Nikolaev AR, Meghanathan RN, van Leeuwen C. 2016. Combining eeg and eye movement recording in free viewing: Pitfalls and possibilities. Brain Cogn. 107:55-83.

Nordhausen K, Ruiz-Gazen A. 2022. On the usage of joint diagonalization in multivariate statistics. Journal of Multivariate Analysis. 188:104844.

Northoff G, Duncan NW, Hayes DJ. 2010. The brain and its resting state activity--experimental and methodological implications. Prog Neurobiol. 92(4):593-600.

Nuzhdin YO. 2019. Resonance-a bci framework for working with multiple data sources. GBCIC; 2019; Graz, Austria.

Nuzhdin YO, Shishkin SL, Fedorova AA, Kozyrskiy BL, Medyntsev AA, Svirin EP, Korsun OV, Dubynin IA, Trofimov AG, Velichkovsky BM. 2017. Passive detection of feedback expectation: Towards fluent hybrid eye-brain-computer interfaces. GBCIC; 2017.

O'Callaghan J. 2024. Apple vision pro: What does it mean for scientists? Nature.

Ovchinnikova AO, Vasilyev AN, Zubarev IP, Kozyrskiy BL, Shishkin SL. 2021. Meg-based detection of voluntary eye fixations used to control a computer. Front Neurosci. 15:619591.

Parra L, Sajda P. 2003. Blind source separation via generalized eigenvalue decomposition. The Journal of Machine Learning Research. 4:1261-1269.

Petrenko MV, Dmitriev SP, Pazgalev AS, Ossadtchi AE, Vershovskii AK. 2021. Towards the non-zero field cesium magnetic sensor array for magnetoencephalography. IEEE Sensors Journal. 21(17):18626-18632.

Pires G, Nunes U, Castelo-Branco M. 2011. Statistical spatial filtering for a p300-based bci: Tests in able-bodied, and patients with cerebral palsy and amyotrophic lateral sclerosis. Journal of neuroscience methods. 195(2):270-281.

Plopski A, Hirzle T, Norouzi N, Qian L, Bruder G, Langlotz T. 2022. The eye in extended reality: A survey on gaze interaction and eye tracking in head-worn extended reality. ACM Computing Surveys (CSUR). 55(3):1-39.

Presacco A, Simon JZ, Anderson S. 2016. Evidence of degraded representation of speech in noise, in the aging midbrain and cortex. Journal of neurophysiology. 116(5):2346-2355.

Protzak J, Ihme K, Zander TO. 2013. A passive brain-computer interface for supporting gaze-based human-machine interaction. Universal Access in Human-Computer Interaction Design Methods, Tools, and Interaction Techniques for eInclusion: 7th International Conference, UAHCI 2013, Held as Part of HCI International 2013, Las Vegas, NV, USA, July 21-26, 2013, Proceedings, Part I 7; 2013: Springer.

Pulvermüller F, Grisoni L. 2020. Semantic prediction in brain and mind. Trends Cogn Sci. 24(10):781-784.

Ramezanpour H, Fallah M. 2022. The role of temporal cortex in the control of attention. Curr Res Neurobiol. 3:100038.

Reddy GR, Proulx MJ, Hirshfield L, Ries A. 2024. Towards an eye-brain-computer interface: Combining gaze with the stimulus-preceding negativity for target selections in xr. Proceedings of the CHI Conference on Human Factors in Computing Systems; 2024.

Riechelmann E, Raettig T, Böckler A, Huestegge L. 2021. Gaze interaction: Anticipation-based control of the gaze of others. Psychol Res. 85(1):302-321.

Rihs TA, Michel CM, Thut G. 2007. Mechanisms of selective inhibition in visual spatial attention are indexed by alpha-band eeg synchronization. Eur J Neurosci. 25(2):603-610.

Risko EF, Richardson DC, Kingstone A. 2016. Breaking the fourth wall of cognitive science: Real-world social attention and the dual function of gaze. Current Directions in Psychological Science. 25(1):70-74.

Sani I, Stemmann H, Caron B, Bullock D, Stemmler T, Fahle M, Pestilli F, Freiwald WA. 2021. The human endogenous attentional control network includes a ventro-temporal cortical node. Nat Commun. 12(1):360.

Särelä J, Valpola H, Jordan M. 2005. Denoising source separation. Journal of machine learning research. 6(3).

Senju A, Hasegawa T. 2005. Direct gaze captures visuospatial attention. Visual cognition. 12(1):127-144.

Shevtsova Y, Yashin A, Vasilyev A, Shishkin S. submitted. Disentangling high-paced alternating i/o in gaze-based interaction.

Shevtsova YG, Vasilyev AN, Shishkin SL. 2023. Machine learning for gaze-based selection: Performance assessment without explicit labeling. 2023; Cham. Springer Nature Switzerland.

Shishkin SL, Kozyrskiy BL, Trofimov AG, Nuzhdin YO, Fedorova AA, Svirin EP, Velichkovsky BM. 2016a. Improving eye-brain-computer interface performance by using electroencephalogram frequency components. Bulletin of Russian State Medical University. (2):36-41.

Shishkin SL, Nuzhdin YO, Svirin EP, Trofimov AG, Fedorova AA, Kozyrskiy BL, Velichkovsky BM. 2016b. Eeg negativity in fixations used for gaze-based control: Toward converting intentions into actions with an eye-brain-computer interface. Frontiers in neuroscience. 10:528.

Siposova B, Carpenter M. 2019. A new look at joint attention and common knowledge. Cognition. 189:260-274.

Stemmann H, Freiwald WA. 2019. Evidence for an attentional priority map in inferotemporal cortex. Proc Natl Acad Sci U S A. 116(47):23797-23805.

Tadel F, Baillet S, Mosher JC, Pantazis D, Leahy RM. 2011. Brainstorm: A user-friendly application for meg/eeg analysis. Comput Intell Neurosci. 2011:879716.

Taulu S, Simola J. 2006. Spatiotemporal signal space separation method for rejecting nearby interference in meg measurements. Phys Med Biol. 51(7):1759-1768.

Tomasello M, Farrar MJ. 1986. Joint attention and early language. Child Dev. 57(6):1454-1463.

Velichkovsky B, Sprenger A, Unema P. 1997. Towards gaze-mediated interaction: Collecting solutions of the “midas touch problem”. Human-Computer Interaction INTERACT’97: IFIP TC13 International Conference on Human-Computer Interaction, 14th–18th July 1997, Sydney, Australia; 1997: Springer.

Xu KZ, Anderson BA, Emeric EE, Sali AW, Stuphorn V, Yantis S, Courtney SM. 2017. Neural basis of cognitive control over movement inhibition: Human fmri and primate electrophysiology evidence. Neuron. 96(6):1447-1458.e1446.

Yang SN, Heinen S. 2014. Contrasting the roles of the supplementary and frontal eye fields in ocular decision making. J Neurophysiol. 111(12):2644-2655.

Zhao DG, Vasilyev AN, Kozyrskiy BL, Melnichuk EV, Isachenko AV, Velichkovsky BM, Shishkin SL. 2021. A passive bci for monitoring the intentionality of the gaze-based moving object selection. J Neural Eng. 18(2):026001.